

32 (Inderbitzin and Subbarao, 2014). *V. dahliae* has an exceptionally wide host range, infecting
33 trees, herbaceous plants, plantation crops, and mushrooms, thriving in subtropical, tropical
34 regions to cold and warm climates.

35 To date, *Verticillium* wilt has been reported in nearly 80 plant genera, affecting more than
36 410 plant species globally (Pegg and Brady, 2002). The pathogen primarily invades plants
37 through the roots, leading to a range of symptoms, including external manifestations such as
38 leaf chlorosis and necrosis, as well as internal vascular discoloration (Chen *et al.*, 2021). The
39 characteristics of the genus *Verticillium*, its role in wilt disease, and methods for its control
40 have been extensively studied (Barbara and Clowes 2003; Faradin and Touma 2006;
41 Klosterman *et al.* 2009). Continued research on its pathogenic mechanisms and resistance
42 strategies remains crucial for managing its widespread impact on agricultural productivity.

43 In eukaryotic cells, eIF4E plays a pivotal role in the initiation and regulation of translation.
44 By interacting with the 5'-cap structure of mRNA and its translation partner, eIF4G, eIF4E
45 facilitates the recruitment of mRNAs to the ribosome (Prevot *et al.*, 2003). The presence of
46 eIF4E, eIF4A, and eIF4G is essential for cap recognition and subsequent RNA helicase
47 activities, which drive efficient protein synthesis (Von der Haar *et al.*, 2004). While the
48 function of eIF4G as a structural scaffold in translation initiation is well-documented, the
49 broader biological significance of eIF4G-related proteins remains largely unexplored. Further
50 evidence from deletion and mutagenesis studies has provided insight into the functional role
51 of the NIC domain within eIF4G. In both yeast (Dominguez *et al.* 1999; Neff and Sachs
52 1999) and human (Imataka and Sonenberg 1997; Morino *et al.* 2000) research has
53 demonstrated that the NIC region is essential for interaction with the helicase eIF4A,
54 underscoring its significance in translation initiation and RNA unwinding mechanisms. To
55 date, the eIF4G family is among the least characterized within eIF4 protein families,
56 warranting further investigation into its molecular mechanisms and functional diversity.

57 Genome-wide sequencing projects have identified the gene families corresponding to each
58 eIF4 factor across various eukaryotic species. To date, two eIF4G proteins have been
59 characterized in humans, namely eIF4G-I (Bradley *et al.*, 2002), and one has been identified
60 in rabbit, eIF4G-I (Lamphear *et al.*, 1993). In plants, wheat possesses two eIF4G proteins
61 (Lax *et al.*, 1985, 1986) along with eIF(iso)4G found in other plants species (Browning *et al.*,
62 1992; Kim *et al.*, 1999). In fungi, *Saccharomyces cerevisiae* contains two eIF4G homologs,
63 eIF4631 and TIF4632 (Goyer *et al.*, 1993), while *Schizosaccharomyces pombe* has a single

64 characterized eIF4G (Hashemzadeh-Bonehi *et al.*, 2003). Additionally, *Drosophila*
65 *melanogaster*, possesses a distinct homolog, Dm-eIF4G (Hernandez *et al.*, 1998).

66 In this study, a partial genomic DNA (gDNA) fragment encoding the N-terminal region of
67 the eIF4G protein from the soilborne fungal pathogen *V. dahliae* was successfully amplified
68 using primers designed through a local alignment search method.

69

70 **Materials and Methods**

71 **Design of degenerate primers**

72 Using the HomoloGene program, protein sequences containing "eukaryotic initiation factor
73 4G" related to the target gene were retrieved. An extensive across multiple organisms
74 identified four fungal sequences from different species in the *Verticillium* genus. These
75 sequences were retrieved from the GenBank database to construct a specialized protein
76 collection database for *V. dahliae* relatives. The maximum e-value accepted in this study was
77 8e-07. Sequences with no homology below this threshold were excluded. Based on the
78 conserved regions identified in the retrieved sequences, two degenerate primers were
79 designed using local alignment search method (Jolodar, 2019).

80

81 **Genomic DNA extraction**

82 *V. dahliae* isolates were cultured on potato dextrose agar (PDA) to promote mycelial growth,
83 following the method described by Yan *et al.* (2022). One hundred mg of mycelium with 300
84 mg of the sterilized sand (white quartz, Sigma) were ground to powder for 30 sec with a
85 pestle in the presence of liquid nitrogen. 600 µl of extraction buffer [100 mM Tris-HCl (pH
86 8.0), 20 mM EDTA, 0.5 M NaCl and 1% sodium dodecylsulfate] was added to the soaked
87 mycelium. The mixture was extracted with equal volumes of phenol/chloroform/isoamyl
88 alcohol (25:24:1) and centrifuged at 12,000 rpm for 5 min. The supernatant was transferred to
89 a new microtube and re-extracted with 400 µl of chloroform. The supernatant was
90 precipitated with 1 volume of ice-cold isopropanol and centrifuged at 12,000 rpm for 10 min.
91 The precipitate was washed with 70% ice-ethanol and was resuspended in 400 µl of TE
92 buffer (10 mM Tris-HCl, 1 mM Na₂EDTA, pH 8.0) containing 20 µg/ml ribonuclease A. The
93 samples were incubated at 37°C for 20 min and then extracted with equal volumes of phenol/
94 chloroform /isoamyl alcohol. The aqueous phase was precipitated by adding 2.5 volumes of
95 ice-cold absolute ethanol and 1/10 volume of 3 M sodium acetate. The samples were then
96 centrifuged at 12,000 rpm for 15 min. The DNA precipitate was washed with ice-cold 70%
97 ethanol, dried and suspended in 100 µl of TE buffer (10mM Tris- HCl, 1mM EDTA). The

98 DNA fragments were visualized on a 1% agarose gel in TAE buffer (40 mM Tris/Acetate, 1
99 mM EDTA) (pH 8.0) at 5 V/cm between positive and negative poles. The gels were stained
100 with 50 µg/ml ethidium bromide and photographed under ultraviolet light. Sterile distilled
101 water was used instead of DNA as a negative control.

102

103 TD-PCR Amplification

104 Degenerate primers were designed on two highly conserved regions identified through a local
105 alignment search method. Using these conserved sequences, two degenerate oligonucleotide
106 primers were designed and synthesized. The forward primer, EIF4-F (5'-
107 GCGgaattcAAYAAYWSAAYAAYATG), corresponding to the protein-coding sequence
108 (NNSNNM), and the reverse primer, EIF4-R (5'-GCGaagcttATRTGNGCNCCNGG), aligns
109 with the protein sequence QPGAHI. In these sequences N, R, W and Y represent nucleotide
110 variations: N (A/G/C/T), R (A/G), W (A/T) and Y (C/T), ensuring primer compatibility
111 across multiple homologous targets. To enhance PCR efficiency and facilitate directional
112 cloning, *EcoRI* and *HindIII* restriction sites were incorporated at the 5' ends of the forward
113 and reverse primers, respectively. Because cleavage sites positioned near the primer ends can
114 result in inefficient digestion by certain restriction enzymes, additional bases (GCG) were
115 appended to the 5' ends. This modification ensures optimal enzyme recognition and effective
116 digestion of the amplified fragments. The restriction enzyme recognition sequences are
117 shown in lowercase letters. TD-PCR reactions were performed under the following
118 conditions: 94°C × 3 min for one cycle. 94°C × 30 s, 42°C × 50 s, 72°C × 1 min for 15 cycles
119 with a 1°C increment per cycle. 94°C × 30 s, 57°C × 50 s, 72°C × 40 s for 20 cycles. Each
120 PCR reaction was performed in a total volume of 25 µl containing 20 mM Tris-HCl, 50 mM
121 KCl, 1.5 mM MgCl₂, 0.2 mM dNTPs of each, 0.5 units of *Taq* DNA polymerase, 0.4 µM of
122 each primer, and 100 ng of genomic DNA. PCR products were loaded on 1% agarose gel
123 containing 50 µg/mL safe stain (Cinagen, Iran) electrophoresis and visualized by UV light.

124

125 DNA sequencing and analysis

126 To determine the sequence of the amplified gene fragments, single bands were purified using
127 an agarose purification kit (Cinagen, Iran) and then sequenced using an Applied Biosystems
128 373 automated sequencer. Nucleotide and amino acid sequences were edited and analyzed
129 using BioEdit software. Primers were designed using Primer3 (Untergasser *et al.*, 2012). The
130 sequences were compared using the BLASTn algorithm from the NCBI Genbank website
131 (ncbi.nlm.nih.gov). The translation of the sequences into amino acids was analyzed using the

132 EXPASY tool program (Gasteiger *et al.*, 2005) (ca.expasy.org/tools/dna.html). Multiple
133 alignments were performed using the CLUSTAL_W program (genome.jp/tools-bin/clustalw)
134 (Thompson *et al.*, 1994) and edited with the BOXSHADE software (Stothard *et al.*, 2000)
135 (bioinformatics.org/SMS/multi_align.html). Phylogeny and genetic distance analysis were
136 performed using the 1000-joining-neighborhood bootstrap test using the MEGA7 software
137 (Tamura *et al.*, 2007). Intron splice sites were determined using NetAspGene -1.0 program
138 (services.healthtech.dtu.dk/services/NetAspGene-1.0/). For obtaining statistical data of
139 proteins, the Gene infinity program was used (org/sms/sms_proteinstats.html).

140

141 Results

142 Design of degenerate primers

143 To identify homologous transcripts in species closely related to *V. dahliae*, the HomoloGene
144 program was utilized within the NCBI GenBank database. The search was performed using
145 the keyword "eukaryotic initiation factor 4G" in the NCBI gene database through the using
146 the BLASTp algorithm. The query was restricted to the *Plectosphaerellaceae* family, which
147 comprises various plant-pathogenic genera and soilborne fungal species. By using this
148 technique, a total of four homologous sequences were identified and retrieved for local
149 alignment, including *V. dahliae* (PNH37575.1), *V. longisporum* (CRK25417.1), *V. alfalfae*
150 (XP_003002440.1) and *V. nonalfalfae* (XP_028490779.1). Degenerate primers were designed
151 based on the sequence numbering of *V. dahliae* (PNH37575.1) targeting amino acid positions
152 between 88-93 for the sense primer and 221-226 for the antisense primers (Figure 1). Two
153 conserved regions, each containing at least six amino acids, were selected as primer-banding
154 sites. These primers were optimized to meet several critical parameters, including appropriate
155 binding temperature, a balanced GC content, prevention of dimenization through self-
156 complementary ends, and minimal secondary structure formation. Since some amino acids
157 are encoded by multiple triplet codons, the primer sequences were designed using IUPAC
158 ambiguity codes to accommodate codon variability. The degeneracy of each primer was
159 determined by multiplying the degeneracy values of the respective amino acids according to
160 the IUPAC coding system. The degeneracy was calculated to be 256-fold for the both primer.



161

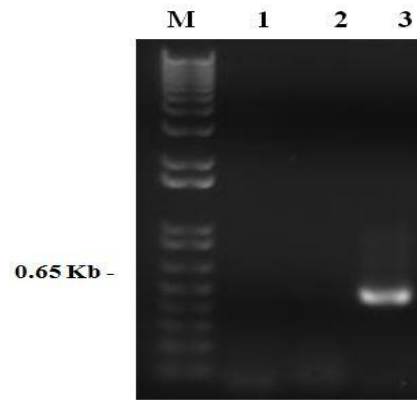
162 **Fig. 1.** Alignments of representative fungus EIF4G protein sequences for designing
 163 degenerate primers. Shading indicates identity (black) or conservative substitutions (grey).
 164 The conserved amino acids for designing degenerate primers are boxed and primer sites
 165 indicated by arrows.

166

167 **TD-PCR amplification of *VdEIF4G***

168 A total of 4 µg of genomic DNA was extracted from 0.5 g of fungal tissue and subsequently
 169 used in polymerase chain reactions. Initially, PCR optimization was conducted using 50 ng of
 170 genomic DNA as the template. A pair of primers was tested under conventional PCR
 171 conditions with an annealing temperature of 58°C; however, no amplification was observed.
 172 To improve results, the genomic DNA concentration was increased, but this adjustment also
 173 failed to produce a positive outcome. Since higher DNA concentration did not enhance
 174 amplification, the TD-PCR technique was implemented. In this method, the PCR reaction
 175 was initiated at an annealing temperature of 42°C for 15 cycles, with a gradual increase of
 176 1°C per cycle, followed by an additional 20 cycles at a final annealing temperature of 57°C.
 177 Using degenerate primers in TD-PCR, a 503 bp fragment, designated as *VdEIF4G* was
 178 successfully amplified.

179



180

181 **Fig. 2.** Agarose gel electrophoresis of PCR products amplified from *V. dahliae* genomic
 182 DNA. Lane M represents the DNA size marker. Lanes 1, 2, and 3 correspond to the following
 183 controls: (1) a negative control using sterile water in place of DNA, (2) a negative control
 184 without *Taq* DNA polymerase, and (3) the PCR-amplified product.

185

186 **Characterization of *VdEIF4G***

187 The amplified *VdEIF4G* gene from *Verticillium dahliae* was confirmed through sequence
 188 analysis. The sequence exhibited a GC content of 62.6%, with nucleotide composition
 189 distributed as 19.3% A, 37.6% C, 25.0% G, and 18.1% T. The amplified fragment was
 190 compared with the NCBI GenBank database using the BLASTn program with the 'highly
 191 similar sequences (megablast)' algorithm. The analysis revealed sequence similarity ranging
 192 from 97.88% to 100%, with matches to the only three incomplete fungal mRNA sequences
 193 from the *Plectosphaerellaceae* family. These included the eukaryotic initiation factor 4F
 194 subunit p130 from *V. dahliae* VdLs.17 (VDAG_06653, XM_009659357.1), an
 195 uncharacterized protein from *V. nonalfalfae*, D7B24_003156 (XM_028637349.1), and the
 196 eukaryotic initiation factor 4F subunit p130 from *V. alfalfae* VaMs.102 (XM_003002394.1).
 197 No genomic sequence similarity was observed. As shown in Figure 3, the amplified genomic
 198 fragment of *VdEIF4G* contained two open reading frames (ORFs), encoding a total of 135
 199 amino acids, separated by a 97-bp intron. **The coding sequence produces a 135-amino-acid**
 200 **protein interrupted by a single intron, with a composition of** aliphatic (35.56%), aromatic
 201 (2.96%), basic (8.89%), and acidic (17.78%) side groups. Among the amino acids, serine
 202 (16.30%), glycine (14.81%), and proline (13.33%) were the most abundant, with 22, 20, and
 203 18 residues, respectively. Further analysis using the Gene Infinity program identified a
 204 glycine-rich domain within the amino acids positioned between residues 30 and 40 (Figure
 205 3), potentially contributing to protein flexibility and functional interactions.

206

```

AAC AAC TCG AAC AAT ATG AAC GGC GCC GGC GAA CAT AGC CGG AAG AGC TCC GTC ACC ATC 61
N N S N N M N G A G E H S R K S S V T I
AGC GCC AAC GGC CCC AAC AGC TAC GCC GGC AAC GGT GGT GCT GCT GGA GGA GGC TCC AAG 121
S A N G P N S Y A G N G G A A G S K
TCC GGT ATC CAG TTC GGC TTC AAG GAC TCG CCT GCC ATC GCC CAC AGC TCG CCC CAG ATG 181
S G I Q F G F K D S P A I A H S S P Q M
TCC GCC GCC CCC ATC CCC ATT CCT GGT GGC AAC CAG AGC GCC AGG GTC CCG TCT CCC GCG 241
S A A P I P I P G G N Q S A R V P S P A
CAC TCT CCC TCC CCC ATC CCC CAG CCC TCT GCC AGT GGT GGT CGT CCC CCT TCG GGC ATT 301
H S P S P I P Q P S A S G G R P P S G I
GCC CAG CAG GGC AAC ATG ACC TTT GGC AGC CTC GGC AGT GAT GGC GATGAgagttttcttgc 365
A Q Q G N M T F G S L G S D G D
gccccccagaaaagacgtttttgtctccccaagatgcgtattttctcaagaaggccctgagctaacgatagtctgtgcac 444

AGCGT CAC ATG AGA CAG GCT CCC ACG CCT CAG AAC CCG GCT GCC CTG GCT TCT CAG CCC 503
R H M R Q A P T P Q N P A A L A S Q P

```

207

208 **Fig. 3.** Displays the nucleotide and predicted amino acid sequences of *VdEIF4G*. Exonic
 209 regions are represented in uppercase letters, while intronic sequences are shown in lowercase.
 210 The donor (GT) and acceptor (AG) sequences at the intron-exon boundaries are highlighted
 211 in bold. Additionally, the putative glycine-rich domain is emphasized using both bold and
 212 underlined formatting to distinguish its position within the sequence.

213

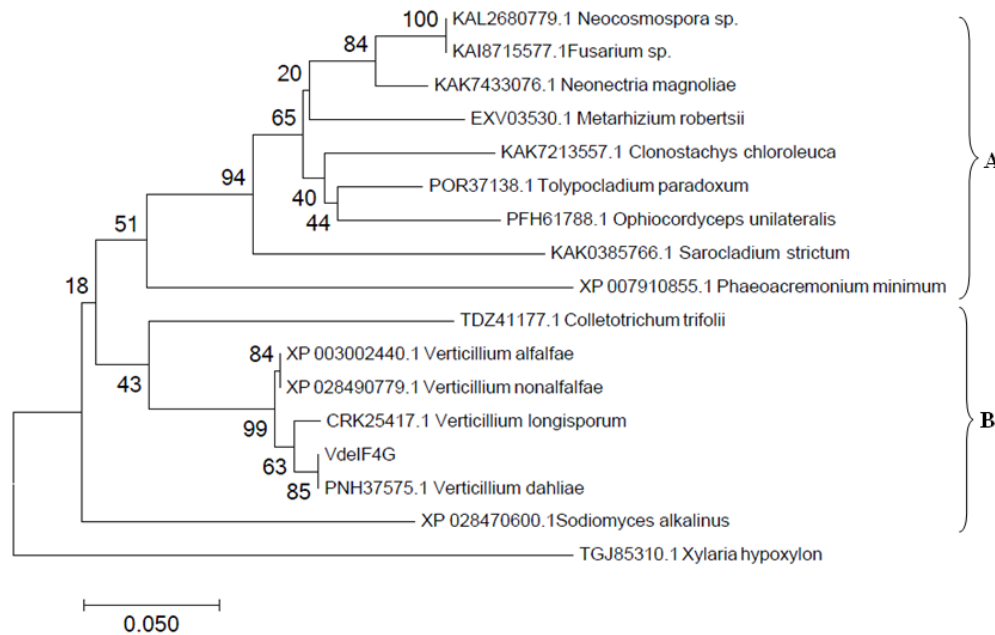
214 In the taxonomic report of *VdEIF4G* at the nucleotide level only showed 3 hits from the
 215 genus *Verticillium* in 81% of overlapping regions with a similarity between 97.99 and 100%.
 216 At the protein level, this report showed a total of 155 hits in the sub-class
 217 *Hypocreomycetidae*, of which 146, 25, and 23 were from the order *Glomerellales*, the family
 218 *Plectosphaerellaceae*, and the genus *Verticillium*, respectively.

219

220 Phylogenetic analysis of *VdEIF4G*

221 To analyze *VdEIF4G* within a broader evolutionary context, phylogenetic analysis was
 222 conducted based on deduced amino acid sequences from *V. dahliae*, along with 15 sequences
 223 from the *Plectosphaerellaceae* family, which includes numerous plant-pathogenic genera and
 224 soilborne fungal species. The constructed phylogram revealed two distinct clusters (A and B).
 225 In Cluster B, *VdEIF4G* was grouped with other *Verticillium* species, supported by a strong
 226 bootstrap score of 99. As expected, *VdEIF4G* exhibited high genetic similarity with various
 227 *eIF4G* homologs within the genus. This evolutionary relationship was confirmed by
 228 comparison with the four available homolog sequences in GenBank from *Verticillium*,
 229 demonstrating that *VdEIF4G* is closely related to *V. longisporum* (CRK25417.1) while
 230 showing slight divergence from *V. alfalfa* (XP_003002440.1) and *V. nonalfalfae*
 231 (XP_028490779.1). Additionally, the sequence of *Colletotrichum trifolii* (TDZ41177.1) was
 232 positioned within a separate sub-cluster, distinct from other *Verticillium* species, supported
 233 by a moderate bootstrap score of 43. Meanwhile, all non-*Verticillium* fungal sequences
 234 belonging to Cluster A were grouped together, with a bootstrap score of 94, indicating a clear

235 phylogenetic separation from *Verticillium* species. *Xylaria hypoxylon* (TGJ85310.1) used as
 236 an out group.



237
 238 **Fig. 4.** Phylogenetic tree constructed from the amino acid sequences of *VdEIF4G* and related
 239 sequences using Neighbor-Joining analysis. Bootstrap values are based on 1,000 replicates,
 240 indicating the statistical support for each branch. Accession numbers corresponding to the
 241 species are listed before their names, representing related gene sequences retrieved from the
 242 GenBank database. The numbers positioned above the branches illustrate the evolutionary
 243 relationships between the grouped sequences.

244
 245 The genetic distance of *VdEIF4G* was calculated using MEGA7 software (Tamura *et al.*,
 246 2007). Among the 13 related protein sequences available in GenBank, *VdEIF4G* exhibited
 247 the lowest genetic distance (1.8%) compared to *V. longisporum* (CRK25417.1) and *V. alfalfa*
 248 (XP_003002440.1).

249
 250
 251
 252
 253
 254
 255
 256
 257
 258
 259
 260
 261
 262
 263
 264
 265

266

267 **Table 1.** Genetic pairwise distances of *VdEIF4G* in comparison to related fungal proteins.

	1	2	3	4	5	6	7	8	9	10	11	12	13
1-VdeIF4													
2-CRK25417.1 <i>V. longisporum</i>	0.01												
3-XP_003002440.1 <i>V. alfalfae</i>	0.01	0.0											
4-TDZ41177.1 <i>C. trifolii</i>	0.17	0.1	0.16										
5-POR37138.1 <i>T. paradoxum</i>	5	75	7										
6-KAL2680779.1 <i>Neocosmospora sp.</i>	0.20	0.2	0.18	0.2	0.1								
7-KAI8715577.1 <i>Fusarium sp.</i>	2	02	4	63	14								
8-XP_028470600.1 <i>Salkalinus strictum</i>	0.18	0.2	0.18	0.2	0.2	0.2	0.2						
9-KAK0385766.1 <i>S. strictum</i>	4	02	4	63	72	46	46						
10-EXV03530.1 <i>M. robertsii</i>	0.25	0.2	0.23	0.2	0.1	0.1	0.1	0.3					
11-XP_007910855.1 <i>P. minimum</i>	4	54	7	98	58	75	75	07					
12-KAK7213557.1 <i>C. chloroleuca</i>	0.20	0.2	0.18	0.2	0.0	0.1	0.1	0.2	0.1				
13-KAK7433076.1 <i>N. magnoliae</i>	2	02	4	46	96	23	23	63	93				
14-PFH61788.1 <i>O. unilateralis</i>	0.28	0.2	0.26	0.2	0.2	0.2	0.2	0.3	0.2	0.2			
	1	63	3	89	54	72	72	07	98	46			
	0.21	0.2	0.20	0.2	0.0	0.1	0.1	0.2	0.1	0.1	0.2		
	1	19	2	72	96	32	32	54	84	32	98		
	0.20	0.2	0.18	0.2	0.0	0.0	0.0	0.2	0.1	0.0	0.2	0.11	
	2	02	4	72	79	61	61	46	67	96	54	4	
	0.22	0.2	0.21	0.2	0.0	0.1	0.1	0.2	0.2	0.1	0.2	0.13	0.1
	8	28	1	63	96	58	58	89	11	23	81	2	23

268

269 **Discussion**

270 *V. dahliae* is a soilborne fungal pathogen that infiltrates host plants through the roots and
271 spreads within the water-conducting tissues, leading to Verticillium wilt. Verticillium wilt
272 symptoms stem from vascular blockage by fungal growth and plant aggregates, with
273 pathogen toxins further driving disease and tissue damage (Fradin et al., 2006). Historically,
274 the symptoms of Verticillium wilt have been attributed to vascular occlusion, caused by the
275 accumulation of fungal mycelia and aggregated plant biomacromolecules. Additionally,
276 phytotoxicity resulting from pathogen-secreted toxins further contributes to disease
277 progression and host tissue damage (Fradin et al., 2006).

278 In this study, the design of degenerate primers enabled the isolation of a partial genomic
279 DNA (gDNA) fragment of the EIF4G gene from *V. dahliae*, utilizing closely related fungal
280 species. To achieve this, degenerate primers were designed based on several known
281 sequences of EIF4G proteins in different fungal species to identify homologous target genes
282 in *V. dahliae*. Generally, designing primers becomes more challenging when the target
283 organism is more distantly related. The primers were constructed based on two blocks of

284 conserved protein sequences that were aligned. For optimal primer design, the conserved
285 regions had to be located in close proximity. The designed primers were required to meet
286 several key criteria, including an appropriate annealing temperature, a suitable GC content
287 range, and non-self-complementary ends to prevent self-complementarity (Kampke *et al.*,
288 2001). Traditional methods for designing degenerate primers utilize software programs such
289 as Gene Fisher (Giegerich *et al.*, 1996), CODEHOP (Rose *et al.*, 2003), and PrimaClade
290 (Gadberry *et al.*, 2005). However, these programs rely on a high degree of sequence
291 conservation across all aligned sequences, which can limit their applicability. In this study,
292 we adopted an alternative approach to identify sufficiently large conserved regions, enabling
293 the design of an effective degenerate primer pair.

294 The careful optimization of the TD-PCR technique was a critical factor in achieving
295 successful amplification using degenerate primers. In this method, the annealing temperature
296 is initially set 5°C below the calculated melting point of the primers to enhance primer-
297 template hybrid formation. Studies have shown that TD-PCR can significantly improve the
298 success rate of degenerate PCR. At lower stringency, annealing facilitates the formation of a
299 greater number of primer-template hybrids. As the PCR cycles progress, the annealing
300 temperature is gradually increased, enhancing specificity and ensuring the amplification of
301 complete primer-template hybrids. This stepwise temperature adjustment improves both
302 efficiency and accuracy in sequence amplification (Scalon *et al.*, 2014)

303 Recent studies have revealed that the physical presence of introns in fungal genomes plays a
304 crucial role in regulating cell survival under starvation conditions (Jo and Choi, 2015;
305 Parenteau *et al.*, 2019). In addition to their regulatory functions, introns serve as hosts for
306 noncoding RNA (ncRNA) genes, including microRNAs and snoRNAs. A genomic survey of
307 *Verticillium dahliae* indicated that 79.3% of its protein-coding genes contain at least one
308 intron, with an average intron length of 100 bp (Muzafar *et al.*, 2021; Jin *et al.*, 2017). In
309 fungal genomes, introns are generally shorter compared to other eukaryotes, with 88–99.8%
310 exhibiting canonical splice sites (GU-AG). In contrast, non-canonical splice sites (GC-AG)
311 are found in 1–2% of introns, while AU-AC splice sites occur in 0.09% of cases (Sieber *et al.*,
312 2018). The annotation of eukaryotic genes, particularly the identification of correct
313 intron-exon structures, remains one of the most complex challenges in genome research
314 (Sharp, 1994). Two primary obstacles in predicting splice sites accurately include: (1) the
315 presence of numerous GT and AG dinucleotides that do not correspond to true splice
316 junctions, leading to false positives, and (2) the occurrence of atypical splice sites, which can

317 result in false negatives (Pucker *et al.*, 2017). Analysis of the *VdEIF4G* genomic sequence
318 confirmed that splicing predominantly follows the GU-AG rule, with the gene interrupted by
319 a 97-nucleotide intron. Intron-exon boundaries were identified through consensus donor-
320 acceptor sequences. Key signals used for this determination include junction sensors, which
321 typically feature a GU dinucleotide sequence signal (C/A)AG/GT(A/G)AGT at the +1/+2
322 position at the 5' end of the intron, and an AG sequence signal (T/C)nN(C/T)AG/G at the 3'
323 splice site (Mount, 1989).

324 Certain amino acids, including glycine, serine, and proline, along with polar and charged
325 residues, are commonly associated with intrinsically disordered proteins (IDPs). These amino
326 acids contribute to structural flexibility and prevent stable folding, allowing proteins to adopt
327 dynamic conformations. Analysis of *VdEIF4G* revealed a high proportion of glycine
328 (14.81%), serine (16.30%), and proline (13.33%), strongly suggesting that it exhibits intrinsic
329 disorder. These residues enhance molecular flexibility; **promote structural flexibility**, and
330 influence protein folding and adaptability. **Additionally, we hypothesize that a glycine-rich**
331 **domain, may be associated with RNA-binding, stress response, and a protein-protein**
332 **interaction especially in fungal pathogens was identified in *VdeIF4G*.** Given its glycine-rich
333 nature and predicted disorder, this protein may play a role in fungal virulence (Nishimura *et*
334 *al.*, 2016), host interactions, or **RNA metabolism** and signal transduction pathways (Mangeon
335 *et al.*, 2010). Further experimental studies, including structural characterization and
336 functional assays, are required to validate its biological significance in *V. dahliae*
337 pathogenicity.

338 In conclusion, degenerate primers designed using a local alignment search method
339 successfully amplified homologous sequences of the eIF4G domain-containing protein from
340 *V. dahliae*.

341 **Acknowledgement**

343 This work was financially supported by research grant from the Vice President of the
344 Research Affairs Office at the Shahid Chamran University of Ahvaz, Ahvaz- Iran.

345 **References**

- 347 1. Barbara, D. J and Clewes, E. 2003. Plant pathogenic *Verticillium* species: how many
348 of them are there? *Mol Plant Pathol.*, **4**: 297-305.

- 349 2. Bradley, C. A., Padovan, J. C., Thompson, J. L., Benoit, C. A., Chait, B. T. and
350 Rhoads, R. E. 2002. Mass spectrometric analysis of the N terminus of translational
351 initiation factor eIF4G-1 reveals novel isoforms. *J. Biol. Chem.*, **277**: 12559-12571.
- 352 3. Browning, K. S., Webster, C., Roberts, J. K. and Ravel, J. M., 1992. Identification of
353 an isozyme from protein synthesis initiation factor 4F in plants. *J. Biol. Chem.*, **267**:
354 10096-10100.
- 355 4. Chen, J. Y., Klosterman, S. J., Hu, X. P., Dai, X. F. and Subbarao, K. V. 2021. Key
356 insights and research prospects at the dawn of the population genomics era for
357 *Verticillium dahliae*. *Annual Review of Phytopathology*, **59**: 31-51.
- 358 5. Dominguez, D., Altmann, M., Benz, J., Baumann, U., Trachsel, H. 1999. Interaction
359 of translation initiation factor eIF4G with eIF4A in the yeast *Saccharomyces*
360 *cerevisiae*. *J. Biol. Chem.*, **274**: 26720–26726.
- 361 6. Fradin, E. F. and Thomma, B. P. H. J. 2006. Physiology and molecular aspects of
362 *Verticillium* wilt diseases caused by *V. dahlia* and *V. albo-atrum*. *Mol Plant Pathol.*,
363 **7**: 71-86.
- 364 7. Gadberry, M. D., Malcomber, S. T., Doust, A. N. and Kellogg E. A. 2005.
365 Prinaclade-a flexible tool to find conserved PCR primers across multiple species.
366 *Bioinformatics*, **21(7)**: 1263-4. doi: 10.1093/bioinformatics/bti134. PMID: 15539448.
- 367 8. Gasteiger, E., Hoogland, C., Gattiker, A., Duvaud, S., Wilkins, M. R. and Appel, R.
368 D.2005. Protein identification and analysis tools on the ExPASy server. In: Walker
369 JM, editor. *The Proteomics Protocols Handbook*. Totowa (NJ): Humana Press; 2005.
370 p. 571-607.
- 371 9. Giegerich, R., Meyer, F. and Schleiermacher C. 1996. GeneFisher-software support
372 for the detection of postulated genes. *Proc. Int. Conf. Intell. Syst. Mol. Biol.* **4**: 68-
373 77(1996). PMID: 8877506.
- 374 10. Goyer, C., Altmann, M., Lee, H. S., Blanc, A., Deshmukh, M. and Woolford J. R.
375 1993. TIF4631 and TIF4632: two yeast genes encoding the high-molecular-weight
376 subunits of the cap-binding protein complex (eukaryotic initiation factor 4F) contain
377 an RNA recognition motif-like sequence and carry out an essential function. *Mol.*
378 *Cell. Biol.*, **13**: 4860-4874.
- 379 11. Inderbitzin, P., Subbarao, K. V. 2014. *Verticillium* systematics and evolution: how
380 confusion impedes *Verticillium* wilt management and how to resolve it.
381 *Phytopathology*, **104**: 564-574.

- 382 12. Hashemzadeh-Bonehi, L., Curtis, P. S., Morley, S. J., Thorpe, J. R. and Pain, V. M.
383 2003. Overproduction of a conserved domain of fission yeast and mammalian
384 translation initiation factor eIF4FG causes aberrant cell morphology and results in
385 disruption of the localization of F-actin and the organization of microtubules. *Genes*
386 *Cells*, **8**: 163-178.
- 387 13. Hernandez, G., Castellano, M. M., Agudo, M. and Sierra, J. M. 1998. Isolation and
388 characterization of the cDNA and the gene for eukaryotic translation initiation factor
389 4G from *Drosophila melanogaster*. *Eur. J. Biochem.*, **253**: 27-35.
- 390 14. Imataka, H. and Sonenberg, N. 1997. Human eukaryotic translation initiation factor
391 4G (eIF4G) possesses two separate and independent binding sites for eIF4A. *Mol.*
392 *Cell Biol.*, **17**: 6940-6947.
- 393 15. Jo, B.S. and Choi, S. S. 2015. Introns: the functional benefits of introns in genomes.
394 *Genomics Inform.*, **13**: 112-8.
- 395 16. Jolodar, A. 2019. Designing of Degenerate Primers-Based Polymerase Chain
396 Reaction (PCR) for Amplification of WD40 Repeat-Containing Proteins Using Local
397 Alignment Search Method. *Journal of Sciences*, **30(2)**:105-111.
398 Doi.10.22059/jsciences.2019.271719.1007349.
- 399 17. Kampke, T., Kieninger, M. and Mecklenburg, M. 2001. Efficient primer design
400 algorithms. *Bioinformatics*. **17(3)**: 214-25. Doi.10.1093/bioinformatics/17.3.214.
401 PMID: 11294787.
- 402 18. Kim, C. Y., Takahashi, K., Nguyen, T. B., Roberts, J. K., and Webster, C. 1999.
403 Identification of a nucleic acid binding domain in eukaryotic initiation factor
404 eIFiso4G from wheat. *J. Biol. Chem.*, 274: 10603-10608.
- 405 19. Klosterman, S. J., Atallah, Z. K., Vallad, G. E., Subbarao, K. V. 2009. Diversity,
406 pathogenicity and management of *Verticillium* species. *Annu Rev Phytopathol.*, **47**:
407 39-62.
- 408 20. Lamphear, B. J., Yan, R., Yang, F., Waters, D., Liebig, H. D. and Klump, H. 1993.
409 Mapping the cleavage site in protein synthesis initiation factor eIF-4 gamma of the 2A
410 proteases from human Cocksackievirus and rhinovirus. *J. Biol. Chem.*, **268**: 19200-
411 19203.
- 412 21. Mangeon, A., Junqueira, R.M. and Sachetto-Martins, G. 2010. Functional diversity of
413 the Plant glycine-rich proteins superfamily. *Plant Signal. Behav.*, **5**: 99-104.

- 414 22. Morino, S., Imataka, H., Svitkin, Y. V., Pestova, T. V. and Sonenberg, N. 2000.
415 Eukaryotic translation initiation factor 4E (eIF4E) binding site and the middle one-
416 third of eIF4GI constitute the core domain for cap-dependent translation, and the C-
417 terminal one-third functions as a modulatory region. *Mol. Cell Biol.*, **20**: 468-477.
- 418 23. Mount, S. M. 1982. A catalogue of splice junction sequences. *Nucleic Acids Res.*, **22**:
419 459-472. Doi:10.1093/nar/10.2.459.
- 420 24. Muzafar, S., Sharma, R. D., Chauhan, N. and Prasad, R. 2021. Intron distribution and
421 emerging role of alternative splicing in fungi. *FEMS Microbiol Lett.*, **26**:
422 368(19):fnab135. Doi: 10.1093/femsle/fnab135. PMID: 34718529.
- 423 25. Neff, C. L. and Sachs, A. B. 1999. Eukaryotic translation initiation factors 4G and 4A
424 from *Saccharomyces cerevisiae* interact physically and functionally. *Mol. Cell Biol.*,
425 **19**: 5557-5564.
- 426 26. Nishimura, T., Mochizuki, S., Ishii-Minami, N., Fujisawa, Y., Kawahara, Y.,
427 Yoshida, Y., Okada, K., Ando, S., Matsumura, H., Terauchi, R., Minami, E. and
428 Nishizawa, Y. 2016. Magnaporthe oryzae glycine-rich secretion protein, Rbfl
429 critically participates in pathogenicity through the focal formation of the biotrophic
430 interfacial complex, *PLoS Pathog*, **12**: e1005921.
- 431 27. Pegg, G. F. and Brady, B. L. 2002. Verticillium wilts. CAB International, Wallingford
432 potato early dying. *Plant Dis.*, **84**: 1241-1245.
- 433 28. Parenteau, J., Maignon, L. and Berthoumieux, M. 2019. Introns are mediators of cell
434 response to starvation. *Nature*, **565**: 612-7.
- 435 29. Rose T. M., Henikoff J. G. and Henikoff S. 2003. CODEHOP (Consensus-Degenerate
436 Hybrid Oligonucleotide Primer) PCR primer design. *Nucleic Acids Res.*, **31(13)**:
437 3763-6. Doi: 10.1093/nar/gkg524. PMID: 12824413.
- 438 30. Scalon M. C, da Silva T. F, Aquino L. C, Carneiro F. T., Lima M. G., Lemos M. D.
439 and Paludo G. R. 2014. Touchdown polymerase chain reaction detection of polycystic
440 kidney disease and laboratory findings in different cat populations. *J Vet Diagn*
441 *Invest.*, **26(4)**: 542-546. Doi: 10.1177/1040638714536561.
- 442 31. Sharp, P. A. 1994. Split genes and RNA splicing. *Cell*, **77(6)**: 805-
443 15. Doi:10.1016/0092-8674(94)90130-9.
- 444 32. Sieber, P., Voigt, K. and Kammer, P. 2018. Comparative study on alternative splicing
445 in human fungal pathogens suggests its involvement during host invasion. *Front*
446 *Microbiol.*, **9**: 2313.

- 447 33. Stothard, P. 2000. The Sequence Manipulation Suite: JavaScript programs for
448 analyzing and formatting protein and DNA sequences. *Biotechniques*, **28(6)**:1102-4.
- 449 34. Tamura, K., Dudley, J, Nei, M. and Kumar, S. 2007. MEGA4: Molecular
450 Evolutionary Genetics Analysis (MEGA) software version 4.0. *Molecular Biology
451 and Evolution*, **24**:1596-1599. Doi.10.1093/molbev/msm092.
- 452 35. Thompson, J. D., Higgins, D. G. and Gibson, T. J. 1994. CLUSTAL W: improving
453 the sensitivity of progressive multiple sequence alignment through sequence
454 weighting, position-specific gap penalties and weight matrix choice. *Nucleic Acids
455 Research*, **22**: 4673-4680. Doi.10.1093/nar/22.22.4673.
- 456 36. Untergasser, A., Cutcutache, I., Koressaar, T., Ye, J., Faircloth, B. C. and Remm M.
457 2012. Primer3—new capabilities and interfaces. *Nucleic Acids Res.*, **40(15)**:e115.
- 458 37. Von der Haar, T., Gross, J. D., Wagner, G. and McCarthy, J. E. G. 2004. The mRNA
459 cap-binding protein eIF4E in post-transcriptional gene expression. *Nat. Struct. Mol.
460 Biol.*, **11**: 503-511.
- 461 38. Yan, N., Addrah, M. E., Zhang, Y., Jia, R., Kang, L. and Zhao J. 2022. Identification
462 and comparison of biological characteristics and pathogenicity of different mating
463 types of *Verticillium dahliae* isolated from potato and sunflower. *Sci Rep.*, **12**:14164.
- 464
- 465
- 466
- 467
- 468
- 469
- 470
- 471
- 472
- 473
- 474
- 475
- 476
- 477
- 478

479 طراحی آغازگرهای دجنره برای افزوده سازی DNA ژنومی رمز گزاری کننده فاکتور شروع ترجمه
480 یوکاریوتی 4 جی *Verticillium dahliae* با استفاده از روش جستجوی همتراز موضعی

481 عباس جلودار

482 چکیده

483 *Verticillium dahlia* یک پاتوژن قارچی خاکی است که باعث بیماری پژمردگی عروقی در بسیاری از گیاهان
484 زراعی و زینتی مهم اقتصادی در سراسر جهان می شود. در این مطالعه، یک قطعه DNA ژنومی که فاکتور شروع
485 ترجمه یوکاریوتی گاما 4 را کد می کند از *V. dahliae* با استفاده از طراحی پرایمرهای دجنره بر اساس روش
486 جستجوی همتراز موضعی افزوده سازی شد. برای شناسایی پروتئین های همولوگ در گونه های نزدیک، پایگاه داده
487 های ژن NCBI با استفاده از برنامه HomoloGene و با استفاده از کلمه کلیدی هدف مورد بررسی قرار گرفت.
488 بخش همتراز توالی های انتخاب شده دو موتیف محافظت را نشان داد که طراحی یک جفت آغازگر دجنره را تسهیل
489 کرد. با استفاده از Touchdown PCR، یک قطعه DNA ژنومی با اندازه 503 نوکلئوتید از *V. dahliae* با موفقیت
490 افزوده سازی و توالی یابی گردید که به عنوان *VdEIF4G* تعیین شد. این قطعه حاوی دو قاب خوانش باز ترجمه
491 (ORFs) بود که در مجموع 135 اسید آمینه را رمزگذاری می کرد، که توسط یک اینترون 97 نوکلئوتیدی از هم جدا
492 می شدند. اتصال اینترون- آگزون در این ژن از قانون GU-AG پیروی می کرد. تجزیه و تحلیل طبقه بندی در سطح
493 نوکلئوتیدی *VdEIF4G* مشابهت با سه توالی موجود در جنس *Verticillium* نشان داد که 81٪ از مناطق همپوشانی
494 را با شباهت توالی بین 97.99 تا 100٪ را پوشش می داد. تجزیه و تحلیل فیلوژنیک در سطح پروتئینی نشان داد که
495 *VdEIF4G* با *V. dahliae* یکسان بود اما، واگرایی از *V. nonalfalfae* و *V. alfalfae* را با کمترین فاصله ژنتیکی
496 بین این دو توالی ها (1.8٪) نشان داد. علاوه بر این، حضور آمینو اسیدهای کوچک و قطبی، همراه با یک دامنه غنی از
497 گلیسین، دخالت بالقوه این پروتئین را در تعاملات بین پاتوژن و میزبان نشان می دهد که ممکن است با حدت
498 بیماریزایی این قارچ در ارتباط باشد. در این مطالعه، آغازگرهای دجنره طراحی شده با استفاده از روش جستجوی
499 همتراز موضعی انجام شدند که به طور موثری توالی های همولوگ پروتئین حاوی دامنه eILF4G مربوطه را از *V.*
500 *dahlia* افزوده سازی نمودند.

501